



Predicting the Shear Strength of Reinforced Concrete Dapped End Beams Using Machine Learning Techniques

Ajibola Ibrahim Quadri ^{1,*}; Agnes Onyeje Ojile ²; Williams Kehinde Kupolati ³; Chris Ackerman ⁴; Jacque Snyman ³; Julius Musyoka Ndambuki ³

1. Ph.D., Department of Civil Engineering, Tshwane University of Technology, South Africa
2. MSc., Department of Civil and Environmental Engineering, The Federal University of Technology, Akure
3. Professor, Department of Civil Engineering, Tshwane University of Technology, South Africa
4. Senior Lecturer, Department of Civil Engineering, Tshwane University of Technology, South Africa

* Corresponding author: quadriai@tut.ac.za

 <https://doi.org/10.22115/scce.2025.480929.1957>

ARTICLE INFO

Article history:

Received: 03 October 2024

Revised: 01 May 2025

Accepted: 30 November 2025

Keywords:

RCDEBs;

Shear capacity;

WEKA;

Support vector machine;

K nearest neighbor;

Multilayer perceptron.

ABSTRACT

Reinforced concrete dapped end beams (RCDEBs) are prone to shear failure due to sudden changes in the cross-section. Hence there is a need to study the shear behavior of the member under loading. This research collected 203 experimental results of RCDEB tests from 17 investigations to predict the shear strength. Geometrical features, concrete strength, amount, and reinforcement layout were considered. The collected datasets were used to train support vector machine (SVM), K-nearest neighbor (KNN), and multilayer perceptron (MLP) models for the shear strength prediction in WEKA software. Variable importance was also carried out to identify the most relevant parameters for predicting the shear strength of RCDEBs. The finding revealed a high prediction accuracy of the shear strength with R of 99, 98, and 97% for SVM, MLP, and KNN, respectively under the percentage split, revealing a strong correlation between the actual dataset and the predicted values. The SVM outperforms MLP and KNN models by 0.52% and 3.27%, respectively. Furthermore, the variable importance analysis revealed that compressive strength, the amount of reinforcement, and geometry are the main parameters influencing the shear capacity of RCDEBs.

How to cite this article: Quadri AI, Ojile AO, Kupolati WK, Ackerman C, Jacque Snyman JS, Ndambuki JM. Predicting the shear strength of reinforced concrete dapped end beams using machine learning techniques. Journal of Soft Computing in Civil Engineering. 2026;10(3):1957. <https://doi.org/10.22115/scce.2025.480929.1957>



1. Introduction

The majority of applications for reinforced concrete dapped end beams (RCDEBs) include parking slots, reinforced concrete buildings, pedestrian bridges, long and short-span bridges, and other reinforced concrete bridge girders [1]. RCDEBs recessed at the end, are held up by corbels, cantilevers, inverted T beams, or columns as shown in Fig. 1. In concrete structures, RCDEBs are mostly used to lower floor levels. Usually used in cantilever span structures, they also function as beam drops between corbels and as discrete beam-to-beam and beam-to-column connections [2]. Using dapped end beams facilitates, assist the assembly of precast concrete structures because they have more lateral stability than isolated beams supported at their bottom faces [3]. Despite these benefits, RCDEBs are considered to be prone to shear failure due to sudden changes in geometry [4,5]. Therefore, it is critical to understand the shear failure of this structural member under loading conditions. RCDEBs can experience an inclined fracture at the service due to the high level of stress at the reentrant corner [6]. Fig. 2 illustrates the different modes of failure of RCDEBs caused by the span-to-depth ratio and internal detailing of reinforcement.

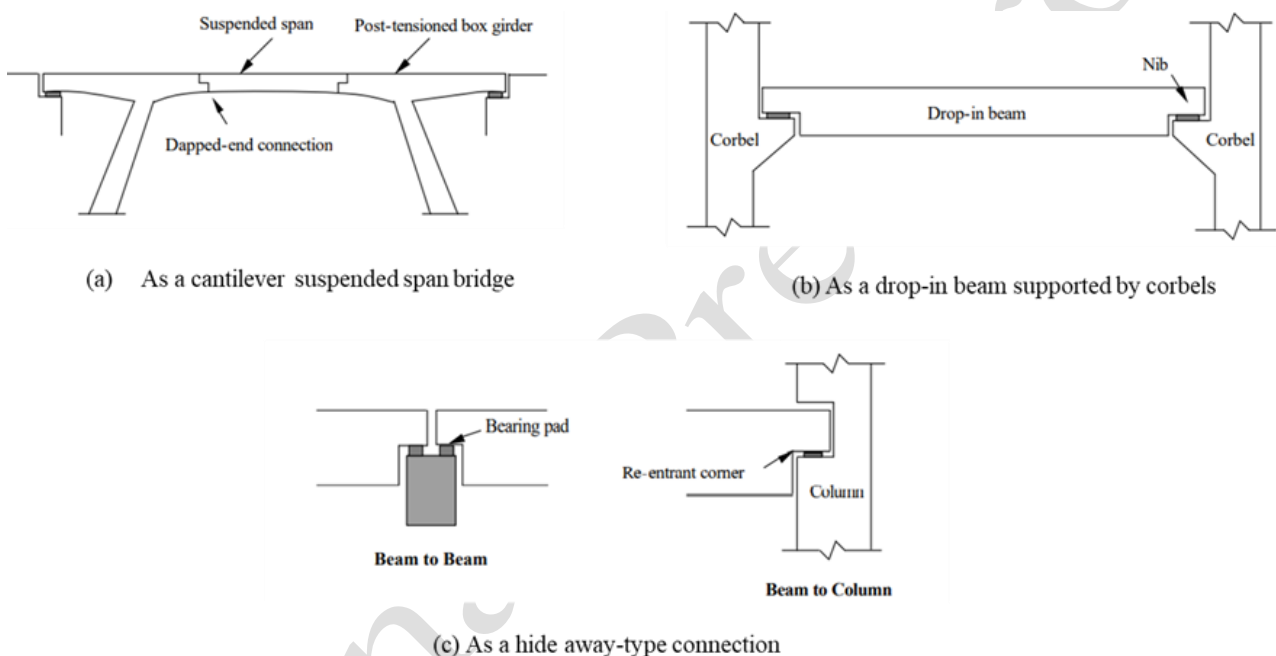


Fig. 1. Different applications of RCDE Bs [7].

The behavior of RCDEBs under different parameters has been investigated in previous years [8–12]. Using the Abaqus software, Melesse et al. [13] studied the geometry characteristics of RCDEBs, including the length of the dapped end, depth of the un-dapped part, and depth of the dapped end. The study reviewed that an increase in the length of the dapped part of the beam resulted in an increase in the beam's deflection and reaction force and that an increase in the depth of the dapped part resulted in a reduction in the maximum deflection and impact stress. Meanwhile, a decrease in the length of the dapped part reduced cracks at the reentrant corner. Reinforcement arrangement and quantity of primary dapped reinforcement have been discovered to have a major effect on the performance of RCDEBs.

The influence of the a/d ratio on the shear strength of RCDEBs was researched by Hussain and Shakir [14] and the span-to-depth ratio (a/d) was observed to affect the shear strength of RCDEB. An increase in a/d reduces the shear strength. A similar result has been achieved by Quadri and Fujiyama [15]. Additionally, Shakir and Alliwe [16] examined the impact of reducing the amount of nib reinforcement and a/d on RCDEBs and discovered that improper detailing nib reinforcement reduced the failure load. Concrete

compressive strength is also a fundamental material property that significantly impacts the performance of RCDEBs [17,18]. A higher compressive strength generally leads to an enhanced overall load-carrying capacity and increased stiffness [19,20]. However, the relationship is not strictly linear, and the influence of compressive strength is often moderated by other factors, such as the type, amount, and arrangement of reinforcement, as well as the loading conditions.

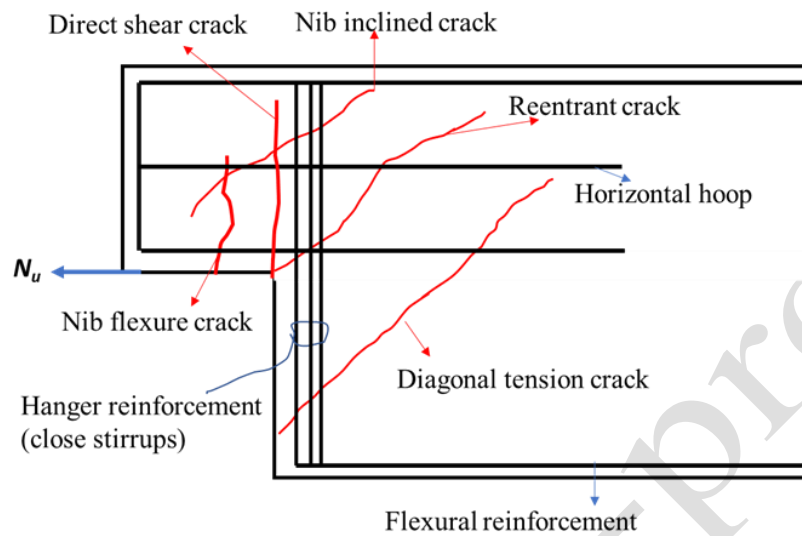


Fig. 2. Failure Mechanism of RCDEBs [21].

Existing design codes, such as ACI 318-08, Eurocode 2, and BS 8110, offer guidance on the design of RCDEBs, but their accuracy in predicting the influence of some parameters; a/d , compressive strength, geometries, etc., may vary significantly [22,23]. Empirical methods, like those presented in the PCI Design Handbook, also exist to predict the shear strength of RCDEBs. Aswin, et al. [22] conducted a comparative study evaluating the accuracy of various codes and empirical methods in predicting the failure loads of RC DEBs. Their analysis revealed that the accuracy of these methods can vary depending on the specific parameters of the DEB and the loading conditions. Some codes may provide conservative estimates, while others may underestimate the actual capacity, particularly for high-strength concrete. The strut-and-tie model (STM) is also a commonly used analytical tool for analyzing DEBs and predicting their strength [24,25]. STM simplifies the complex stress distribution in the dapped-end region by representing it as a system of compression struts and tension ties. While STM offers a relatively simple and intuitive approach, its accuracy can depend on the skill and experience of the analyst in selecting appropriate strut and tie configurations. The limitations of existing design codes and models in capturing the complex interaction between concrete compressive strength and DEB performance highlight the need for further research and refinement of these approaches. The development of more accurate and reliable predictive models is crucial for ensuring the safe and economical design of DEBs, especially those made using high-strength concrete. Furthermore, the development of design guidelines specifically addressing the unique challenges posed by high-strength concrete in DEBs is needed.

One of the approaches adopted by researchers recently in predicting the shear capacity of reinforced concrete structures is the use of machine learning (ML). This has gained application in structural and material engineering aspects, as they have been proven to provide a good predictive model [26,27]. In research by Ma et al. [28] used six ML models to predict the shear strength of reinforced concrete deep beams and evaluated their results against five earlier closed-form models. 457 datasets on deep beams with or without web reinforcements were used to develop the machine learning model. Badra et al. [25] estimated the punching shear strength of fiber-reinforced polymer-reinforced concrete slabs without shear

reinforcement using ANN and SVM algorithms. The ANN and SVM models had respective RMSE values of 3.06, 1.10 kN, and 1.32 kN. The performance of the ANN was better when compared to the performance measures of the SVM model. Mogahed [29] used models: Gaussian, Random Forest, SVR, ANN, LightGBM, XGBoost, CatBoost, and symbolic regression. ML model hyperparameters were tuned using the Bayesian optimization approach to assess the predictive power of ML techniques for the shear strength of reinforced concrete deep beams. It was reported ML models are highly reliable and accurate compared to conventional models. ML approaches have also been adopted for predicting the compressive strength of concrete, with high accuracy reported [30–35]. Concrete strength is affected by the shape and size of aggregates, the water-cement ratio [36]. The effect of the water-cement ratio on concrete compressive strength using different ANNs has been predicted accurately [37]. Lin and Wu [38] adopted the Back Propagation (BP) with a single hidden layer network considered in the ANN model to predict the compressive strength of concrete from existing experimental work and proposed formulae for predicting the compressive strength of concrete. Moradi et al. [39] reported a good correlation between the experimental and predicted compressive strength of Metakaolin using ANN, it was observed that the surface area and the ratio of silicate and aluminate in the pozzolan influenced the compressive strength. The dynamic response of a two-dimensional steel frame has also been predicted using the ML approach, and high accuracy has been reported [40].

The appraisal of the literature reveals that a single criterion, such as hanger reinforcement, a/d ratio, or concrete strength, among others, is inadequate to evaluate whether or not the shear capacity performance of RCDEBs may be enhanced under sustained loading. Several features must be combined to create a satisfactory shear capacity. ML could be a suitable approach to mapping the relationship between the parameters and the shear strength. The main objective of this research is to check the suitability of using the ML method for predicting the shear strength of RCDEBs utilizing the test results previously reported in the literature as the input dataset. Prediction of the shear capacity of RCDEBs using machine learning techniques does not exist in the literature thus far like other uniform cross-section beams which can be easily predicted with existing data. The authors selected three ML algorithms; Support vector machine (SVM), K-nearest neighbor (KNN), and Multilayer Perception (MLP) using Waikato Environment for Knowledge Learning (WEKA) software. WEKA has been adopted to predict the strength of concrete [41–43]. It is noted that KNN could be biased toward predicting more complex values especially when nonlinear instances are involved. The authors extend the algorithm to SVM and MLP which could handle such cases and compare the accuracy. The findings of this investigation will enhance the understanding of the shear strength of RCDEBs by exploring several parameters like the geometrical features, strength of materials, amount, and layout of reinforcement which may reduce the need for studies of each pair of parameters. The information from this investigation can also be used in the preliminary design and selection of features of RCDEBs which will be an economical and time-safe approach to designing RCDEBs.

2. Shear strength estimation of dapped end beams

Several researchers have made proposals on the shear response of RCDEBs to the applied load. Concrete compressive strength, aggregate interlock action, and resistance of reinforcement to stresses are important for the shear performance of RCDEBs [44,45]. Werner [46] proposed the shear that causes a diagonal tension crack to propagate at the reentrant region of RCDEBs. The nominal shear strength, V_u , at the reentrant end of RCDEBs is expressed in Equation (1).

$$V_u = V_c + V_s + V_h \quad (1)$$

The shear carried by the shear reinforcement, V_s , is expressed in Eq. (2) as;

$$V_s = A_v f_y \left(1 - \frac{d}{2a}\right) \quad (2)$$

V_h is the shear carried by the longitudinal reinforcement at the tension zone. Mattock and Chan [47] modified the V_h as given in Equation (3).

$$V_h = A_h f_y (1.5 - a/d) \quad (3)$$

The shear carried by the plain concrete is contributed by the compressive strength as expressed in Equation (4).

$$V_c = (3.5d/a)bd \sqrt{f'_c} \quad (4)$$

3. Methodology

3.1. Description of ML proposed algorithms with WEKA

WEKA provides a robust framework for exploring machine learning's efficacy in forecasting shear strength. It outperforms existing methods by allowing algorithms to learn the complicated correlations between parameters affecting structural shear strength (e.g., geometry, a/d , reinforcement) and compressive strength straight from data. WEKA includes a wide range of algorithms, such as linear regression for simple relationships, ensemble methods like Random Forest that use multiple models to improve accuracy, and instance-based learning with k-Nearest Neighbors, which allows for predictions for new mixes by comparing them to existing data points [48]. The WEKA suite is divided into 3 different graphical (Fig. 3) interfaces namely; the Explorer, Experimenter, and the Knowledge Flow. It has been proven as good software for ML development and has been used in several studies in structural engineering [49–52].



Fig. 3. Graphical Interface of WEKA [53].

3.1.1. Support vector machine (SVM)

SVM is a supervised ML technique excellent at determining optimal decision borders, generally depicted as hyperplanes as shown in Fig. 4. The equation of the decision boundary is impacted by the support vectors, which are the samples closest to it, and the margin reflects the spacing between the hyperplane and these vectors [54]. SVM can handle more complex regression (SVR) and classification problems under nonlinear

cases with high-performance [55]. This investigation utilized SVR since the datasets consist of continuous variable [23,56].

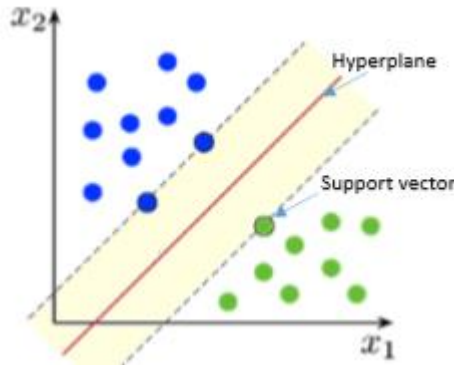


Fig. 4. Support Vector Machine [57].

For SVR the algorithm used an intense loss function to maintain the maximum margin. The linear model of the intense loss function is expressed in Equation (5) [58].

$$L_{\varepsilon} = (y - f(x, w)) = \begin{cases} 0 & \text{if } |y - f(x, w)| \leq \varepsilon \\ |t - f(x, w)| - \varepsilon & \text{otherwise} \end{cases} \quad (5)$$

Where L_{ε} is a loss function, y is the actual value of the input and ε is an error $f(x, w)$ is the linear model in the feature space.

The model output is represented in Equation (6)

$$f(x) = \sum_{i=1}^n (a_i^* - a_i) K(x_i, x_j) + b \quad (6)$$

Where $[a_i]^*$ and a_i are weight coefficients, $K(x_i, x_j)$ and b is the bias [50]. PUK is used for this investigation because it can handle the nonlinear behavior of reinforced concrete structures and the complexity involved. Other kernel functions fail to provide satisfactory results [59]. Thus, leveraging PUK can enhance the model performance prediction of RCDEBs.

3.1.2 K-nearest neighbor (KNN)

Regression and classification applications may both benefit from the flexibility of the k-nearest neighbors (KNN) technique, which takes as input k-training samples that are the closest to the target data point in a given data collection [51,60]. The number of neighbors K is the core deciding factor. A case is classified by a majority vote of its k nearest neighbors measured by the distance function. The various types of distance measures used in KNN are expressed in Equations (7-9) [53].

$$Euclidean = \sqrt{\sum_{i=1}^k (x_i - y_i)^2} \quad (7)$$

$$Manhattan = \sum_{i=1}^k |x_i - y_i| \quad (8)$$

$$Minkowski = [\sum_{i=1}^k (|x_i - y_i|^q)]^{1/q} \quad (9)$$

For regression, the output value is computed by the average of K closest neighbors value as expressed in Equation (10).

$$f(x) = \frac{1}{k} \sum_{i=1}^k y_i \quad (10)$$

Instance-Based Classifier (IBK) on Weka was used in this investigation to develop the KNN model[37]. The distance function and the numbers of K were varied to achieve the best parameters for the model. K of 1, 3, 5 ... 11, with an increment of 2 was used for the hyperparameter tuning and Euclidean distance functions were set as the default for the algorithm's performance. The distance function evaluates the closeness or otherwise the predicted value to the actual value. In this case, several distance functions such as Chebyshev, Manhattan, Filtered, and Minkowski were also tested for optimal performance.

3.1.3. Multilayer perceptron (MLP)

MLP is a supervised ML algorithm in the form of neural network architecture that uses backpropagation to classify instances [44,51]. A neural network is a computer model made of many neurons or nodes linked to one another [20]. As seen in Fig. 5, MLP networks are comprised of a minimum of three layers: an input layer, an output layer, and one or more hidden layers. Every layer in the MLP comprises several nodes and one or more processing units (neurons), all of which are completely linked to units in layers above it. The first layer that the feature vector passes through is called the input layer. The input layer in this investigation has 14 nodes that include the input parameters for the generated model. The hidden layer consists of one or more layers of threshold logic units, which make up the second layer. The number of hidden layers and neurons was chosen by tuning the number of nodes until the optimal model was achieved. This layer's objective is to transform the information into content that the output layer can utilize to predict the data. Finally, the output layer, which consists of a single node, represents the predicted value, namely, the predicted shear strength of RCDEBs.

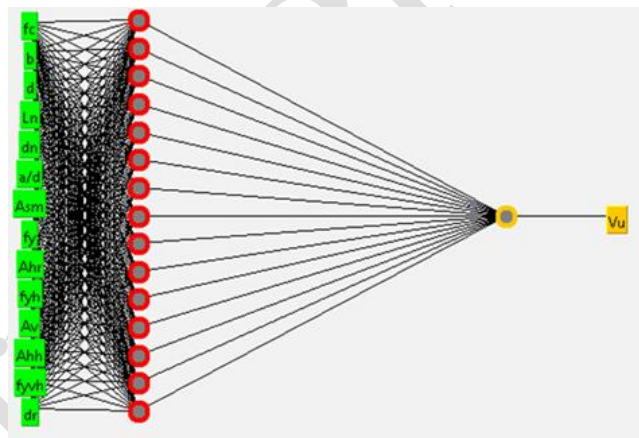


Fig. 5. Multilayer Perceptron.

The output of a neuron is as expressed in Equation (11):

$$\text{Output of a neuron} = \sum_{n=1}^N W_n X_n + b \quad (11)$$

Where X_n is the input W_n is the weight of the output X_n and b is the bias

3.2. Description of dataset

In this investigation, 203 datasets were collected from test results of 17 experimental research on RCDEBs. The research included 12 test results from Lu et al. [60], 24 test results from Lu et al. [41], 24 test results from Lu et al. [3], 24 test results from Wang et al. [61], 8 test results from Mattock and Chan [47], 8 test results from Rajakpse et al. [6], 26 test results from Falcon et al., [7], 18 test results from Hezinger [23], 4 test results from Almed et al. [56], 3 test results from Aswin et al. [60], 5 test results from Shakir and Allawe

[16], 6 test results from Aksoylu et al. [10], 8 test results from Aswin et al. [62], 6 test results from Muhammed and Abbas [46] 4 test results from Peng [63], 15 test results from Mohammed et al. [20] and 8 test results from Liem [64]. The fourteen features selected as the input variables to predict the shear strength of RCDEBS are the compressive strength of concrete (f_c), the width of the beam (b), depth of the beam (d), Span to depth ratio (a/d), nib length (L_n), nib depth (d_n), area of main steel reinforcement (A_{ms}), yield strength of main reinforcement steel (f_y), area of horizontal reinforcement (A_h), yield strength of horizontal reinforcement (f_{yh}), area of vertical reinforcement (A_v), area of hanger reinforcement (A_{hh}), yield strength of hanger reinforcement (f_{yhh}), diagonal reinforcement (A_{dr}). These are the main parameters reported to influence the performance of RCDEBs. This prediction did not include other parameters such as the total length of the beam. The output variable is the ultimate shear strength of RCDEBs. Table 1 provides a statistical description of the dataset utilized. The input variables include the primary input factors that influence the shear performance of RCDEB. The input parameters' mean, standard deviation, minimum, and maximum values are provided in detail, which are suitable for understanding the dispersion of the range of the dataset for reliable and accurate prediction. Stages of data processing for this work are presented in the appendix. As shown in Fig. 6. a/d negatively impacts the data, however, it is one of the indispensable parameters reported to affect the shear strength performance [10,17,23,52,65]. The inclined reinforcement (A_v) was not adopted by some of these authors (see attached data set) although using it increases the performance of RCDEBs, it does not affect the performance of the model.

Table 1

Statistical Description of the Dataset.

Attributes	Mean	Standard Deviation	Minimum value	Maximum Value
f_c (Mpa)	38.464	12.878	16.01	69.2
b (mm)	199.596	57.566	120	350
d (mm)	501.547	175.457	250	1000
L_n (mm)	334.453	160.578	110	650
d_n (mm)	257.488	92.547	100	500
a/d	1.485	0.703	0.52	3.3
A_{ms} (mm ²)	569.616	451.762	0	2000
f_y (MPa)	444.074	139.639	0	633
A_h (mm ²)	133.337	151.389	0	567.1
f_{yh} (MPa)	261.470	206.987	0	575
A_v (mm ²)	199.964	228.651	0	992.4
A_{hh} (mm ²)	491.378	445.753	0	2712
f_{yhh} (MPa)	425.740	147.339	0	425.74
A_{dr} (mm ²)	84.870	222.341	0	1257
V_u (kN)	268.289	208.468	11.07	1046

3.3. Data preprocessing and testing

During the preprocessing stage, the dataset was normalized. Normalization is the process of transferring a dataset from a high value to a low value equivalent. The normalized data falls within the range of 0 and 1[66]. The normalization is expressed in Equation (12).

$$x_{normalized} = \frac{x - x_{minimum}}{x_{maximum} - x_{minimum}} \quad (12)$$

where $x_{normalized}$ is the normalized outcome, x is the value to be normalized in the selected dataset, $x_{minimum}$ and $x_{maximum}$ is the minimum and the maximum value in the selected dataset.

After normalization, the dataset was partitioned for training and testing set. The training set was used for training the regression model while the testing set was used for validating the model. A percentage split of 80% for training and 20% for testing was recorded as the best partition of the dataset for a percentage split [67]. The splitting was done automatically on the WEKA software using the Explorer/classify interface. Cross-validation was also used for partitioning to improve the partitioning process and also for comparing with percentage split.

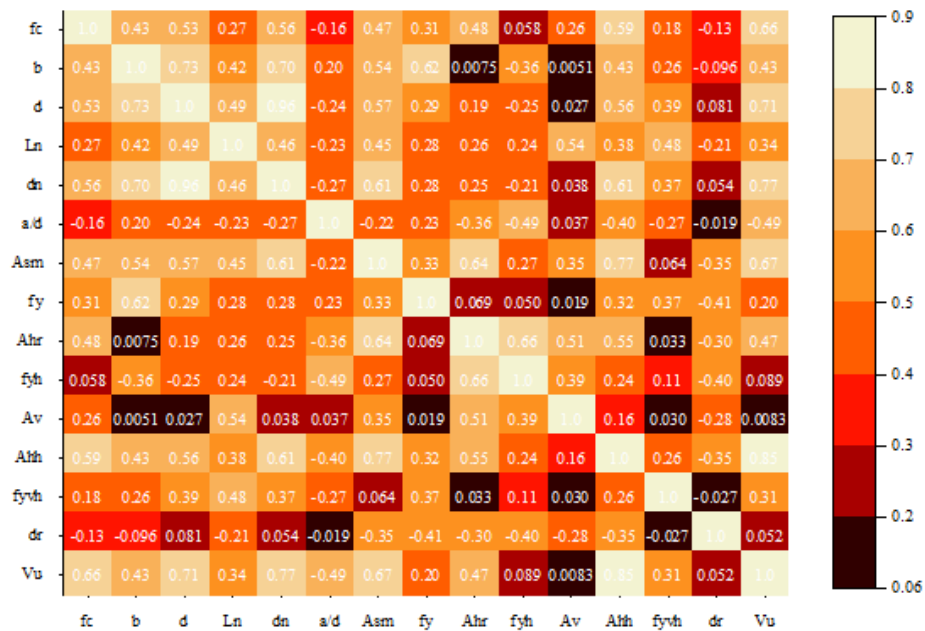


Fig. 6. Correlation Matrix for the Input and Output Parameters.

3.4. Optimization of hyperparameters for ML algorithms

Hyperparameters that could have an impact on the performance of most ML algorithms are first established before the training is performed. The hyperparameter tuning was carried out for the percentage split and cross-validation process used in this investigation. For the SVM model, two parameters were tuned; the kernel function and the regularization parameter (C) [55]. The default kernel type used for SVM in WEKA is poly-kernel and the value of the regularization parameter is 1. For optimization, the kernel was changed first while the regularization parameter C was held constant after that, the regularization parameter was varied within the range from 1 to 10 using the optimum kernel function. The kernel function can easily handle the nonlinear behavior of concrete under variable loading, while the regularization parameter can allow control over the trade-off through normalization. In the MLP, three parameters were varied, and their default values were Seed (0), Hidden Layers (a), and Learning Rate (0.3). To obtain higher accuracies, the parameters were tuned, and their accuracies were analyzed. The seed parameter and learning rate of the MLP model were also tuned, and variations in the model's performance were observed.

3.5. Model evaluation

The performance of the investigated ML model in predicting the shear strength of RCDEBs was evaluated based on test data through statistical metrics, i.e., correlation coefficient (R), mean absolute error (MAE), root mean squared error (RMSE), relative absolute error (RAE) and root relative squared error (RRSE)) to investigate the statistical relation between original data and predicted data [49].

A statistical measure of the relationship between predicted and actual values is the correlation coefficient (R) [68], expressed in Equation (13):

$$R = \frac{\sum_{i=1}^n (A_i - \bar{A})(P_i - \bar{P})}{\sqrt{\sum_{i=1}^n (A_i - \bar{A})^2} \sqrt{\sum_{i=1}^n (P_i - \bar{P})^2}} \quad (13)$$

Where; A is the actual value, P is the predicted value, \bar{A} is the mean of the actual value, \bar{P} is the mean of the predicted value and n is the number of observations.

Root Mean Square Error (RMSE) measures the discrepancies between the values predicted by a model and the values observed. The RMSE is as expressed in Equation (14) [68]:

$$RMSE = \sqrt{\frac{1}{n} \sum_{i=1}^n (P_i - A_i)^2} \quad (14)$$

Mean Absolute Error (MAE) is a measure of the set of predicted values to real values, or the degree to which a predicted model closely resembles an actual model [43]. This is expressed in Eq. (15) as;

$$MAE = \frac{1}{n} \sum_{i=0}^n |P_i - A_i| \quad (15)$$

The degree of deviation between the predicted and actual values is shown by the Root Relative Squared Error (RRSE) and Root Absolute Error (RAE). RAE and RRSE are expressed in Equations (16) and (17):

$$RAE = \frac{\sum_{i=1}^n |P_i - A_i|}{\sum_{i=1}^n |\bar{P} - A_i|} \quad (16)$$

$$RRSE = \sqrt{\frac{\sum_{i=1}^n (P_i - A_i)^2}{\sum_{i=1}^n (\bar{P} - A_i)^2}} \quad (17)$$

4. Results and discussion

4.1. Result of hyperparameter optimization

This section delves into determining the appropriate value of hyperparameters that have a major influence on the selected model and result in the best performance in estimating RCDEB shear strength.

The correlation coefficient was chosen as the performance measure for selecting the most promising machine learning algorithm parameter for predicting the shear strength of RCDEBs. The default kernel type used for SVM in WEKA is the poly-kernel type at a regularization parameter, C, of 1 which generated R of 0.9606 and 0.963 for cross-validation and percentage split, respectively, was achieved. The C was then increased to 3, 5, 7..., 11 by intervals of 2 to get C that gives an optimal value of R. This is to actualize the best value when other kernels are used. In this case, C of 3 gave an optimum value. Figs. 7 and 8 show the result of tuning the kernel parameter and the regularization parameter for optimum accuracy for prediction. There is no improvement in C beyond 3 as seen in Figure 7, indicating 3 as the best C for predicting the accuracy of the distance functions. In Figure 8, the Pearson Universal Kernel (PUK) with C value 3 was chosen as the optimal hyperparameter because it achieved the highest R of 1.41% and 3% more than the accuracy of the default parameter for cross-validation and percentage split respectively. The Radial Basis Function Kernel (RBFK) and the normalized poly kernel (Fig. 8) performed lower than the default by 4.6% and 4%, respectively. Demonstrating unsuitability in matching the complexity in the nonlinearity among the concrete parameters. This implies that the PUK kernel is more suitable for mapping the nonlinear

relation between the input and the output data to predict the shear strength of RCDEBs. The RBFK centers more on closer datasets, however, when the nonlinearity is large due to the far distance, the performance decreases. PUK has also been adjudged more effective in predicting concrete structures' strength [69–71].

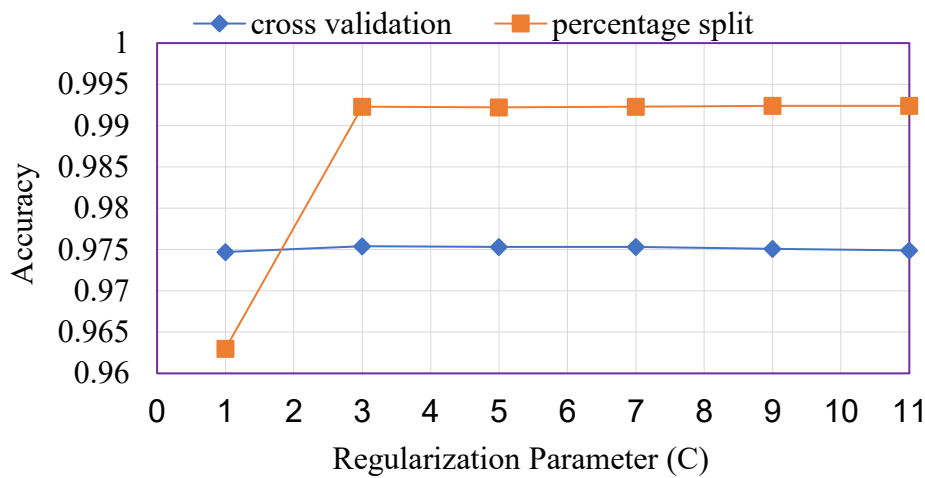


Fig. 7. Tuning the Regularisation Parameter.

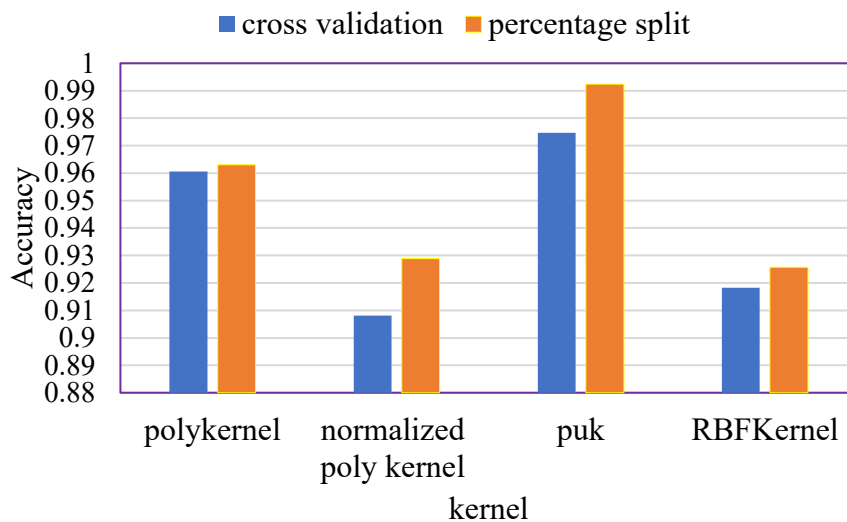


Fig. 8. Comparison of the selected distance functions.

For the KNN algorithm, the default nearest neighbor and hyperparameters in WEKA are a K value of 1 and the distance function is Euclidean distance. The distance functions are the hyperparameters that help understand how close or otherwise the predicted value is to the actual value. These two default parameters achieved R of 0.9508 and 0.9563 for cross-validation and percentage split respectively. Figs. 9 and 10 show the result of manipulating the distance function and numbers K for optimal accuracy. The k value of 3 achieved the highest R for both the cross-validation and the percentage split as shown in Figure 9. With this optimum value, other distance functions such as Manhattan and Minkowski distance, etc. as presented in Fig.10 are also tuned in to have the best accuracy, The accuracy of Chebyshev distance in predicting the shear strength is lesser than the default by 1.7% for the cross-validation, and by 3.1% for the percentage split, implying that it could not predict like others, while other distances performed better than the default with accuracy close to 1 suggesting the distance between the predicted values and the actual are close. The Manhattan distance gave the best prediction of the shear strength by ensuring the similarity between the data points is appropriately measured in the models relying on distance metrics. The normalized features

correlate strongly with the predicted shear strength. It is 1.3% higher than the default distance for the percentage split and by 1% for the cross-validation.

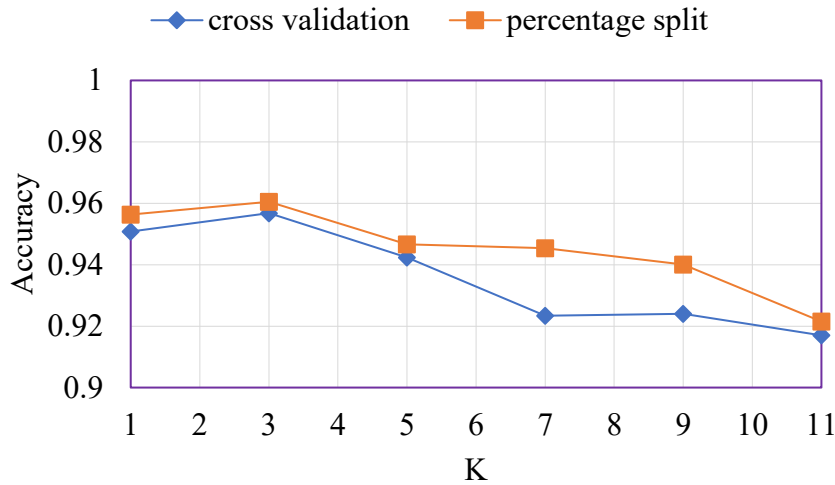


Fig. 9. Tuning of k value for KNN model.

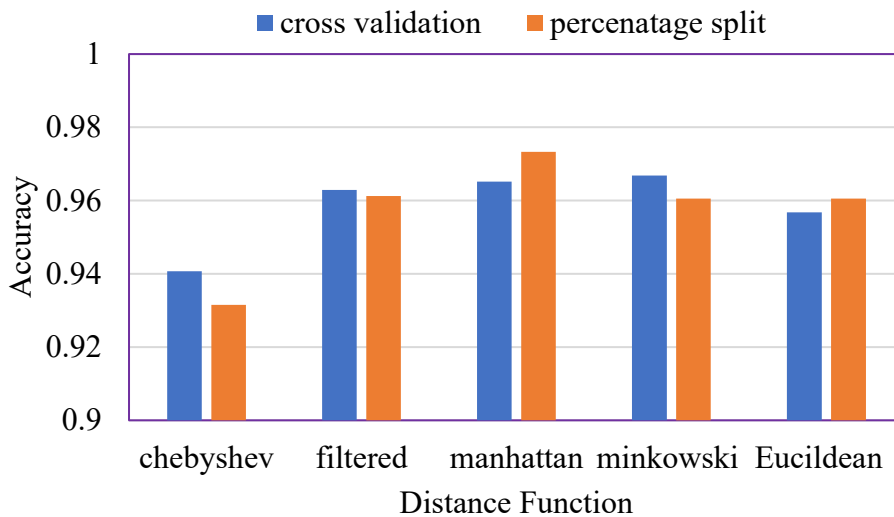


Fig. 10. Tuning the Distance Function.

Figure 11 depicts the performance of an MLP model with different hidden layers. Hidden layers i, t, and a (14, 15, and 7 nodes, respectively) outperformed hidden layer "o" (two nodes). This is because more neurons in the hidden layer can capture the complex relationship occurring in the nonlinear relation in the datasets making the prediction more accurate. For cross-validation, the accuracy of all hidden layers was attained using a seed value of 150, as shown in Fig. 12a. However, for the percentage split, the accuracy was recorded at various seed values, as shown in Figure 12b. This variance could be because cross-validation measures the model's effectiveness across multiple dataset subsets, whereas percentage split focuses on the proportion allotted for validating the model. According to Fig. 13a, each hidden layer achieved the best accuracy at different learning rates for 10-fold cross-validation, however for a percentage split, the highest accuracies for all hidden layers were reached at 0.3 learning rate, as shown in Fig. 13b. It is observed that the cross-validation quickly reached the optimum performance in seeding and learning rate (Figs 12a and 13a), implying that convergence was reached early. This affects the training stage, yielding lower performance predictions of the shear strength of RCDEBs (see Fig. 11). Although different seeds yield slightly different results, assigning a percentage dataset to the neuron can ensure that RCDEB test

data are repeatable. Thus, by leveraging hidden layers and seeding for nonlinear modeling and reproducibility, a more robust and accurate model for predicting the shear strength of RCDEBs can be built

Across all models used, the percentage split outperformed cross-validation. The datasets for forecasting shear strengths were divided in a manner that favored the training and testing sets. The testing set provided a robust representation of the dataset, allowing the datasets to be produced swiftly and with high accuracy, however, cross-validation had subsets that resulted in low enhancement in some folds, resulting in a drop in average performance. Furthermore, unlike cross-validation, the percentage split approach does not introduce variability across different data divides. However, the cross-validation method of splitting datasets is more reliable for model performance because it requires repeated training and testing on different subsets of data.

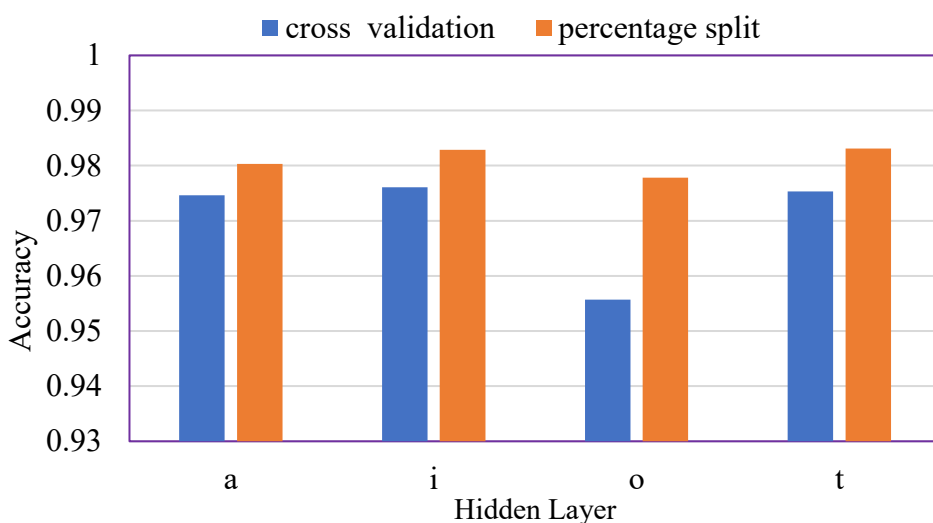


Fig. 11. Tunning the Hidden Layer.

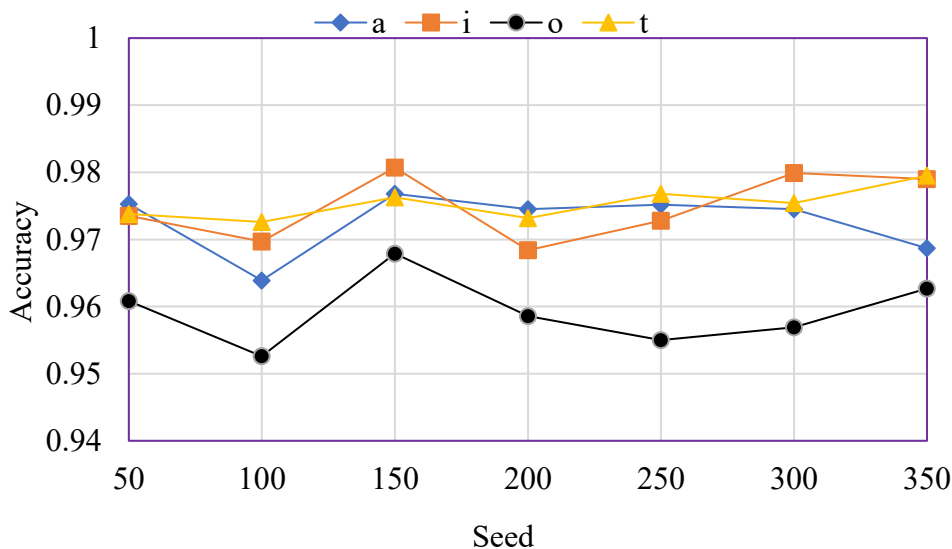


Fig. 12a. Tunning the seed parameter (cross-validation)

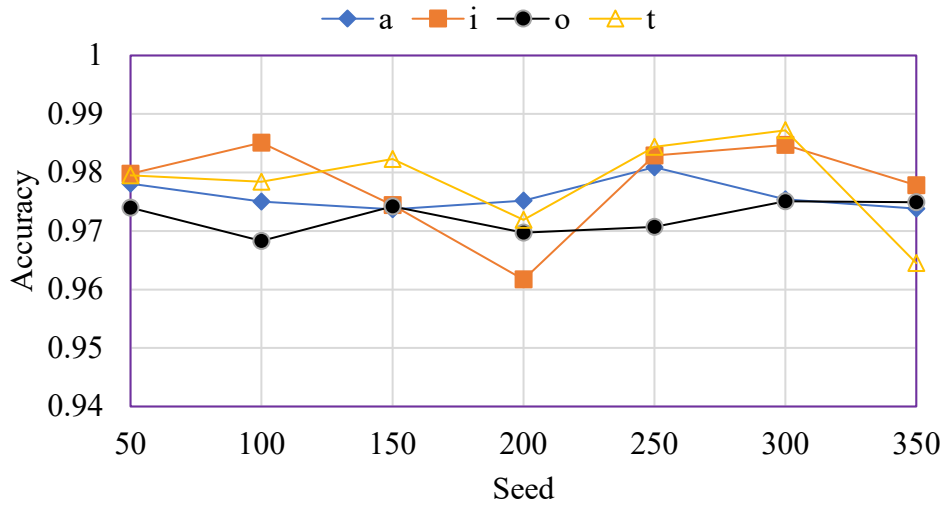


Fig. 12b. Tuning of Seed Parameter for MLP Model (Percentage Split).

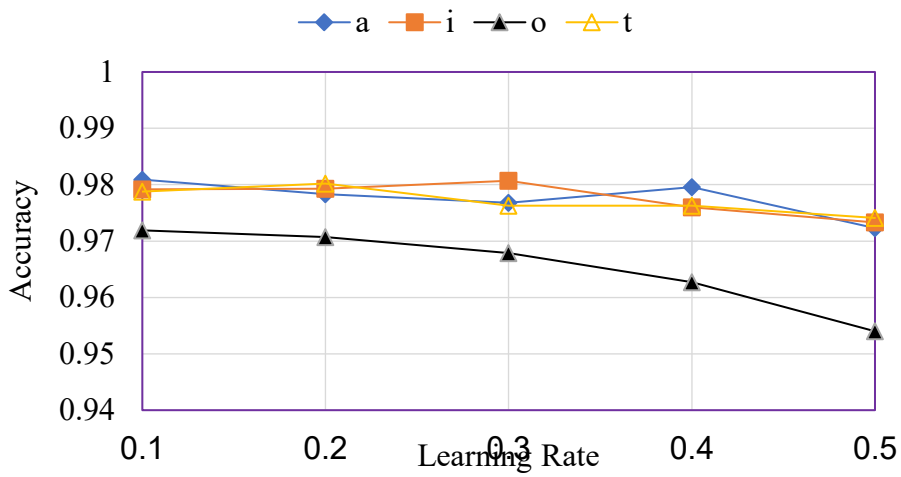


Fig. 13a. Learning Rate Value and their Performance (cross-validation).

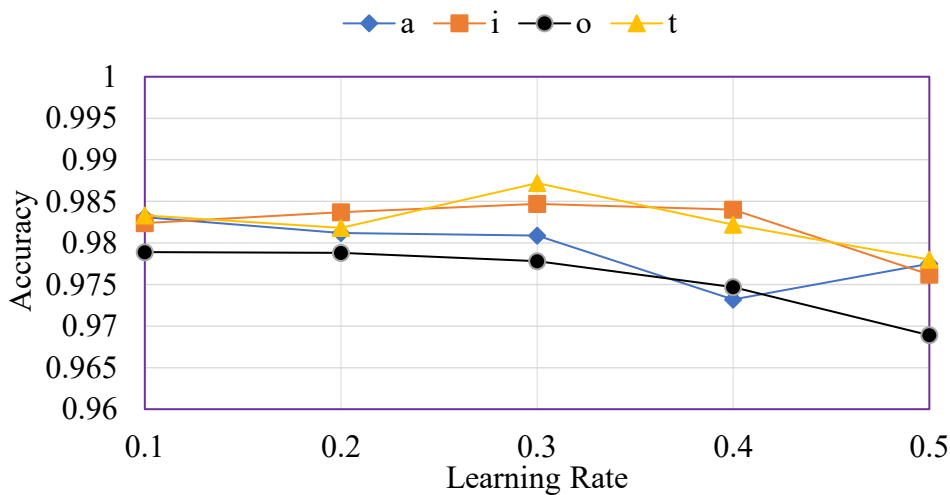


Fig. 13b. Learning Rate Value and their Performance (percentage split).

After tuning the hyperparameters for the ML algorithms, Table 2 summarizes the selected hyperparameters for the SVM, KNN, and MLP models for predicting the shear strength of RCDEBs. These parameters can be adapted to real-life estimation of the shear strength of RCDEBs and can also be extended to predict the shear strength of structures with abrupt changes in cross-sections.

Table 2

Optimum hyperparameter for ML models.

ML model	Optimum hyperparameter cross-validation	Optimum hyperparameter Percentage split
SVM	C=3, kernel = PUK	C=3, kernel =PUK
KNN	K=3 distance function Makowski	K=3 distance function = Manhattan
MLP	Number of hidden layers =1, number of neutrons in the hidden = 14, seed =150, learning rate 0.3	Number of hidden layers =1, number of neutrons in the hidden = 15, seed =300, learning rate 0.3

4.2. Comparison between the performance of the different ML models

The accuracy of the developed ML models in predicting the shear strength of RCDEBs has been evaluated. Tables 3 and 4 present the statistical comparison of the three algorithms employed in predicting the shear strength of RCDEBs using the percentage split and cross-validation. The developed ML models have R close to 1.0 and a small value of MAE, RMSE, RAE, and RRSE. These metrics ensure that the model predictions are accurate, reliable, and safe for structural engineering applications and for making appropriate design decisions. In Table 3, the SVM model best fits the experimental shear strength of RCDEBs, with values 0.52% and 3.27% greater than the MLP and KNN models, respectively. The difference between MAE and RMSE for SVM is negligible, indicating that it is less sensitive to outliers. These errors are more substantial in KNN than in other algorithms, highlighting the possibility of overfitting. A look at the standard deviation (see Table 1) revealed that the data had a significant variance around the mean. This could potentially influence KNN accuracy. RAE and RRSE are very low, demonstrating that SVM can correctly forecast the nonlinear effect problem associated with RCDEBs.

The cross-validation approach was also used to assess the ML models' resilience across various dataset subsets. Ten folds of the data were separated; K-1 (9) folds constituted the training set, while one-fold served as the test set. Table 4 shows the performance of the ML algorithms using the cross-validation method. The R values of the ML models varied between 0.9568 to 0.9807. These values are within an acceptable range, indicating that the developed algorithms perform well in predicting the values of shear strength of RCDEBs. MLP model outperforms the rest in terms of having the highest R values and the lowest values for MAE, RMSE, RAE, and RRSE, among all models examined for cross-validation. The values of these metrics range between 1 (100%) and 0 (0%).

Table 3

Statistical characteristics of the SVM, KNN, and MLP model using the analyzed testing set.

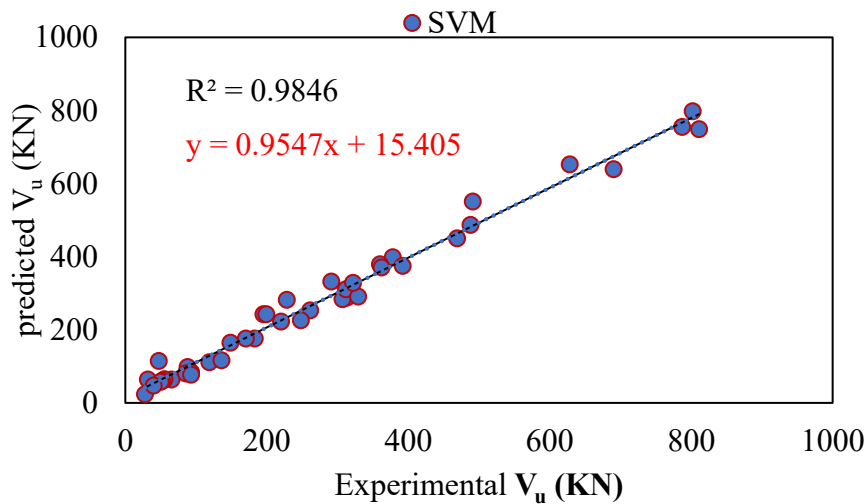
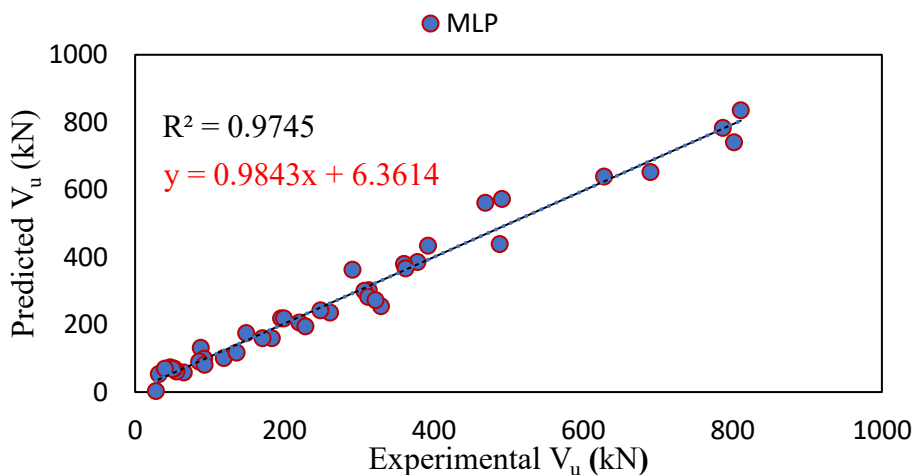
Performance Measure	SVM	KNN	MLP
R	0.9924	0.9605	0.9872
MAE (kN)	20.9261	40.6753	27.1506
RMSE (kN)	27.3613	61.7584	35.0208
RAE (%)	12.2107	23.7347	15.8428
RRSE (%)	12.5077	28.2317	16.0092

Table 4

Statistical characteristics of the SVM, KNN, and MLP model using 10 fold cross validation.

Performance Measure	SVM	KNN	MLP
R	0.9754	0.9568	0.9807
MAE (kN)	25.8664	39.3127	29.5184
RMSE (kN)	46.6134	60.7746	41.3986
RAE (%)	16.086	24.4481	18.3571
RRSE (%)	22.2865	29.0572	19.7933

Figs. 14 to 16 represent the SVM, KNN, and MLP models' scatter plots of the predicted and actual shear strength of RCDEBs. These plots are made from the data present in the evaluated testing dataset. The ML models' data points exhibit a good agreement between model expectations and experimental findings, as they are grouped closely. The coefficient of determination, R^2 , for the shear strength of RCDEBs experimental and predicted outcomes for the SVM, MLP, and KNN models are 0.9846, 0.9745, and 0.9474, respectively, which are excellent values demonstrating the competence of the models to predict the shear strength. SVM performed best among the models, the points are tightly clustered around the diagonal line demonstrating the ability of the SVM algorithm to predict values that align well with the experimental value than MLP and KNN.

**Fig. 14.** Scatter Plot of Experimental and Predicted Shear Strength of RCDEBs for SVM Model.**Fig. 15.** Scatter Plot for Experimental and Predicted Shear Strength for MLP Model.

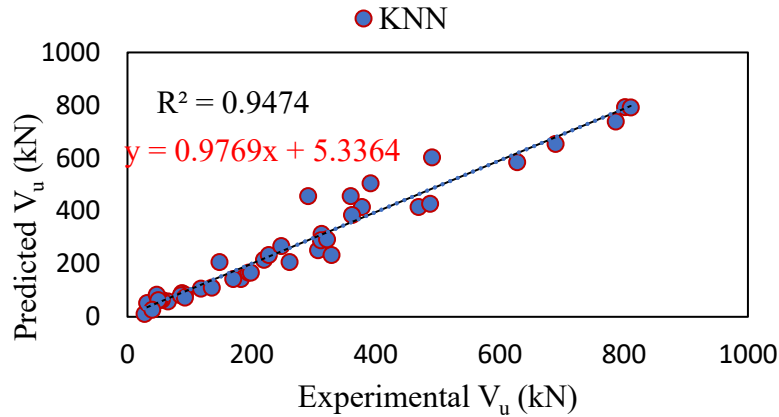


Fig. 16. Scatter Plot for Experimental and Predicted Shear Strength for KNN Model.

4.3. Sensitivity analysis of features

The shear strength of reinforced concrete beams is developed from the compressive strength of concrete, aggregate interlock, and reinforcement provision [72]. These constitute the evaluated input parameters for the shear performance of RCDEBs. Fig. 17 shows the values of the 14 most essential parameters for estimating RCDEB shear strength with variable importance (VI). This variable importance was tuned in the WEKA select attribute section using the ‘Correlation Attribute Eval’. As can be observed, each feature has varying degrees of influence on shear strength development. Nevertheless, the hanger reinforcement area (A_{hh}), the depth of the nib (d_n), the effective depth of the beam (d), the area of the main reinforcement area (A_s), and the compressive strength (f_c), contribute to the most to the shear strength of RCDEBs. The variable importance evaluation also confirmed that predicting the RCDEB's shear strength requires not only compressive strength and reinforcement but also the geometry of the dapped end such as the cross-section. The inclined reinforcement area (A_v) and the shear span to depth ratio a/d are observed here as unimportant parameters. Researchers have reported that loading at a/d less than unity increases the shear strength of RCDEBs [14,23,52]. This is also reflected in this prediction as a/d greater than unity dominates the dataset.

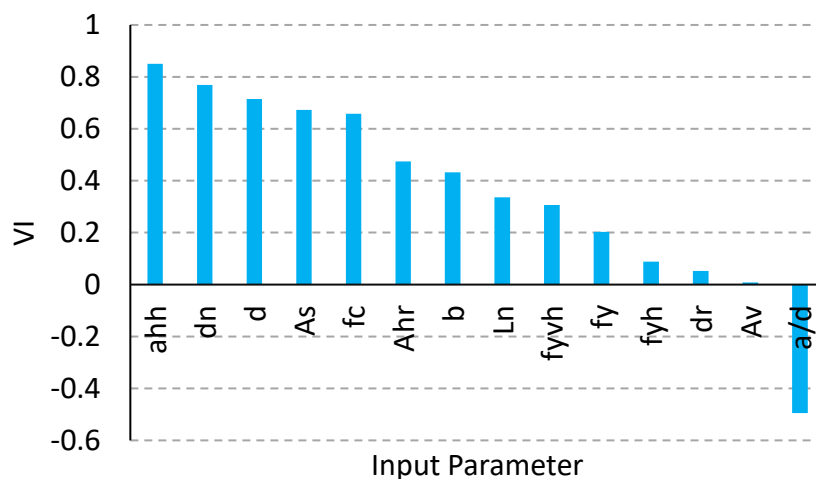


Fig. 17. Sensitivity of input parameter to the shear strength of RCDEB.

5. Conclusions

This investigation collected 203 datasets from different research papers on experimental investigations of the shear strength of RCDEBs. Three ML models; SVM, KNN, and MLP were adopted using WEKA. R,

MAE, RMSE, RAE, and RRSE were used to assess these models' performance. The following is a summary of the conclusions drawn from the results of the analysis:

- The optimal value for the regularization parameter, C, was 3 for cross-validation and percentage split. Tuning this value to the kernel functions in SVM produced the best prediction in PUK, which could predict the complexity involved in RCDEB shear strength with correlation coefficient R accuracy of 99% and 97% for percentage split and cross-validation, respectively.
- Increasing the default hyperparameter in KNN resulted in an ideal value of 3, which offered the best prediction of shear strength of 97% and 96% in the Manhattan distance function. For MLP, cross-validation performed best at lower seed and learning rates than the percentage split, resulting in a reduced prediction capacity of shear strength among the hidden layers.
- The three algorithms used to forecast the shear strength of RCDEBs are extremely accurate. SVM produced the highest prediction accuracy, followed by MLP, while KNN produced the lowest prediction. The RAE, RRSE, MAE, and RMSE for measuring the accuracy of the test model were higher in KNN than others, with a high prediction accuracy of shear strength indicating potential overfitting. However, SVM has lower values, showing that it can handle the nonlinearity associated with RCDEB's shear capacity.
- The variable importance analysis demonstrated that the compressive strength of the concrete, the reinforcement, and the shape of the reinforced concrete dapped end beams are critical parameters for increasing shear capacity. Loading at a shear span-to-depth ratio (a/d) greater than unity has a negative effect on the shear strength.

Funding

This research received no external funding.

Conflicts of interest

The authors declare no conflict of interest.

CRedit authorship contribution statement

Ajibola Ibrahim Quadri: Conceptualization, Data curation, Formal analysis, Investigation, Methodology, Resources, Validation, Writing – original draft.

Agnes Onyeje Ojile: Conceptualization, Data curation, Formal analysis, Investigation, Methodology, Resources, Writing – original draft.

Williams Kehinde Kupolati: Conceptualization, Project administration, Software, Supervision, Visualization, Writing – review & editing.

Chris Ackerman: Data curation, Resources, Validation, Writing – review & editing.

Jacque Snyman: Methodology, Software, Supervision, Visualization, Writing – review & editing.

Julius Musyoka Ndambuki: Investigation, Project administration, Software, Supervision, Writing – review & editing

Appendix

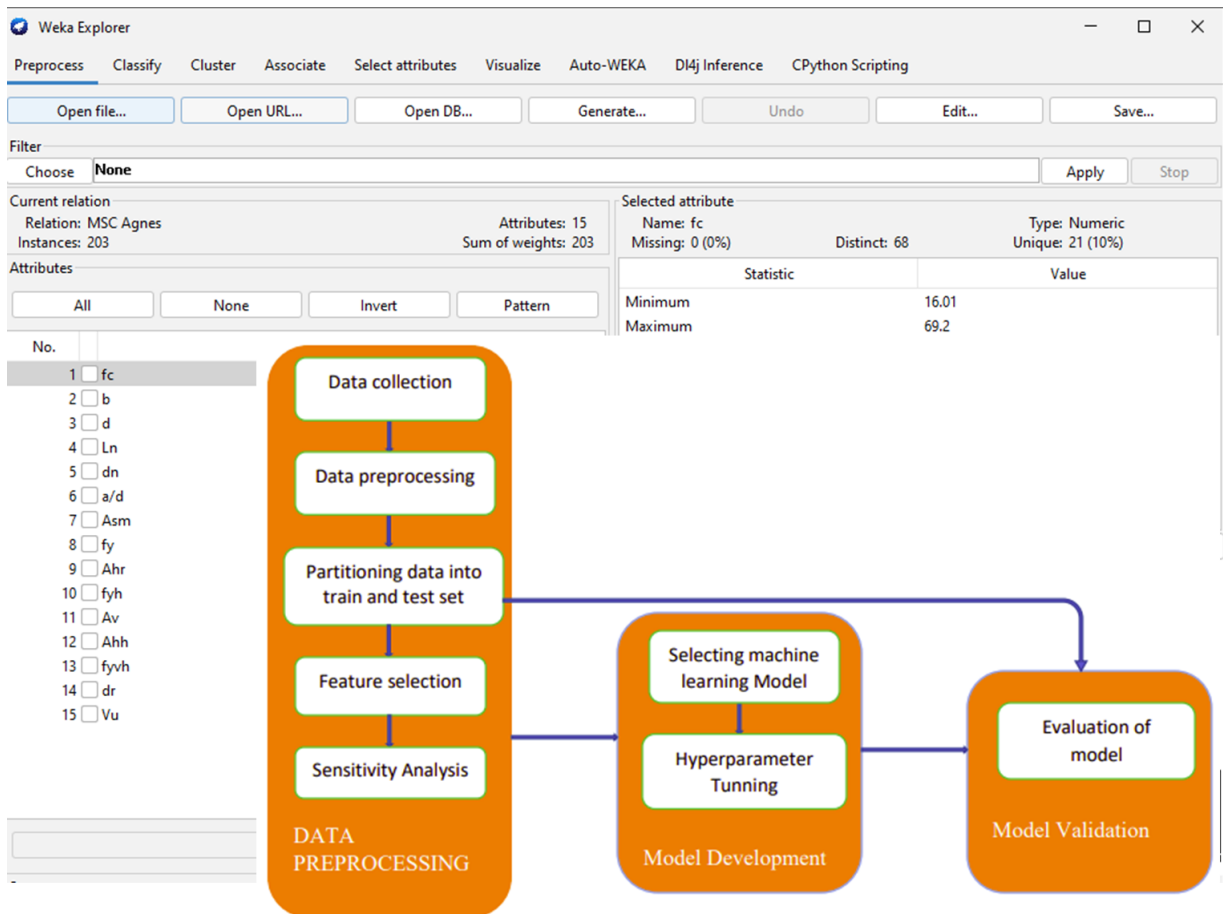


Fig. Data Processing and Evaluation stage.

References

- [1] Aksoylu C, Özkılıç YO, Arslan MH. Damages on prefabricated concrete dapped-end purlins due to snow loads and a novel reinforcement detail. *Eng Struct* 2020;225:111225. <https://doi.org/10.1016/j.engstruct.2020.111225>.
- [2] Yang K-H, Ashour AF, Lee J-K. Shear strength of reinforced concrete dapped-end beams using mechanism analysis. *Mag Concr Res* 2011;63:81–97. <https://doi.org/10.1680/mac9.000006>.
- [3] Lu W-Y, Chen T-C, Lin I-J. Shear strength of reinforced concrete dapped-end beams with shear span-to-depth ratios larger than unity. *J Mar Sci Technol* 2015;23:5.
- [4] di Prisco M, Colombo M, Martinelli P, Coronelli D. The technical causes of the collapse of Annone overpass on SS. 36. *Calcestruzzo Strutt. Oggi Teor. Impieghi Mater. Tec.*, ITA; 2018, p. 1–16.
- [5] Cook WD, Mitchell D. Studies of Disturbed Regions Near Discontinuities in Reinforced Concrete Members. *ACI Struct J* 1988;85. <https://doi.org/10.14359/2772>.
- [6] Rajapakse C, Degée H, Mihaylov B. Assessment of Failure along Re-Entrant Corner Cracks in Existing RC Dapped-End Connections. *Struct Eng Int* 2021;31:216–26. <https://doi.org/10.1080/10168664.2021.1878975>.
- [7] Mata-Falcón J, Pallarés L, Miguel PF. Proposal and experimental validation of simplified strut-and-tie models on dapped-end beams. *Eng Struct* 2019;183:594–609. <https://doi.org/10.1016/j.engstruct.2019.01.010>.
- [8] Masénas V, Meškénas A, Valivonis J. Analysis of the Bearing Capacity of Reinforced Concrete Dapped-End Beams. *Appl Sci* 2023;13:5228. <https://doi.org/10.3390/app13095228>.
- [9] Hussain HA, Shadhan KK. The Effect of Construction Joint on Behavior of Reinforced Concrete Dapped End Beam. *J Phys Conf Ser* 2021;1973:012030. <https://doi.org/10.1088/1742-6596/1973/1/012030>.

- [10] Aksoylu C, Özkılıç YO, Arslan MH. Experimental and numerical investigation of shear strength at dapped end beams having different shear span and recess corner length. *Structures* 2023;48:79–90. <https://doi.org/10.1016/j.istruc.2022.12.076>.
- [11] Di Carlo F, Meda A, Molaioni F, Rinaldi Z. Experimental evaluation of the corrosion influence on the structural response of Gerber half-joints. *Eng Struct* 2023;285:116052. <https://doi.org/10.1016/j.engstruct.2023.116052>.
- [12] Quadri AI, Fujiyama C. Cyclic Shear Response of Reinforced Concrete Dapped-End Beams (RCDEBs) Under Bond Deterioration. *Int. PhD Symp. Civ. Eng., n.d.*, p. 227.
- [13] Melesse G, Behailu T, Kaske Kassa H. Finite Element Analysis of a Reinforced Concrete Dapped-End Beam under the Effects of Impact Velocity and Dapped-End Beam Cross-Section Geometry. *Adv Mater Sci Eng* 2023;2023:1–13. <https://doi.org/10.1155/2023/5869552>.
- [14] Hussain HN, M. Shakir Q. Experimental Study of the Behavior of Reinforced Concrete Beams with Composite Dapped End under Effect of Static and Repeated Loads. *Int J Appl Sci* 2019;2:p43. <https://doi.org/10.30560/ijas.v2n1p43>.
- [15] Quadri AI, Fujiyama C. Response of Reinforced Concrete Dapped-End Beams Exhibiting Bond Deterioration Subjected to Static and Cyclic Loading. *J Adv Concr Technol* 2021;19:536–54. <https://doi.org/10.3151/jact.19.536>.
- [16] SHAKIR QM, Alliwe R. Upgrading of deficient disturbed regions in precast RC beams with near surface mounted (NSM) steel bars. *J Mater Eng Struct «JMES»* 2020;7:167–84.
- [17] Lu W-Y, Lin I-J, Yu H-W. Behaviour of reinforced concrete dapped-end beams. *Mag Concr Res* 2012;64:793–805. <https://doi.org/10.1680/mac.11.00116>.
- [18] Atalla A, ALjebouri K. Parameters Affecting the Strength and Behavior of RC Dapped-End Beams: A Numerical Study. *J Eng* 2022;28:78–97. <https://doi.org/10.31026/j.eng.2022.10.06>.
- [19] Quadri AI, Ali K. Numerical Appraisal of Reinforced Concrete Dapped-End Girder Under High-Fatigue Fixed Pulsating and Moving Loads. *Transp Res Rec J Transp Res Board* 2024;2678:257–78. <https://doi.org/10.1177/03611981231184176>.
- [20] Mohammed BS, Aswin M, Liew MS, Zawawi NAWA. Structural Performance of RC and R-ECC Dapped-End Beams Based on the Role of Hanger or Diagonal Reinforcements Combined by ECC. *Int J Concr Struct Mater* 2019;13:44. <https://doi.org/10.1186/s40069-019-0356-x>.
- [21] Quadri AI. Behavior of disturbed region of RC precast beams upgraded with near surface mounted CFRP fiber. *Asian J Civ Eng* 2023;24:1859–73. <https://doi.org/10.1007/s42107-023-00605-5>.
- [22] Aswin M, Syed ZI, Wee T, Liew MS. Prediction of Failure Loads of RC Dapped-End Beams. *Appl Mech Mater* 2014;567:463–8. <https://doi.org/10.4028/www.scientific.net/AMM.567.463>.
- [23] Herzinger R, Elbadry M. Alternative Reinforcing Details in Dapped Ends of Precast Concrete Bridge Girders. *Transp Res Rec J Transp Res Board* 2007;2028:111–21. <https://doi.org/10.3141/2028-13>.
- [24] Menichini G, Gusella F, Orlando M. Methods for evaluating the ultimate capacity of existing RC half-joints. *Eng Struct* 2024;299:117087. <https://doi.org/10.1016/j.engstruct.2023.117087>.
- [25] Desnerck P, Lees JM, Morley CT. The effect of local reinforcing bar reductions and anchorage zone cracking on the load capacity of RC half-joints. *Eng Struct* 2017;152:865–77. <https://doi.org/10.1016/j.engstruct.2017.09.021>.
- [26] Tapeh ATG, Naser MZ. Artificial Intelligence, Machine Learning, and Deep Learning in Structural Engineering: A Scientometrics Review of Trends and Best Practices. *Arch Comput Methods Eng* 2023;30:115–59. <https://doi.org/10.1007/s11831-022-09793-w>.
- [27] Fakharian P, Nouri Y, Ghanizadeh AR, Safi Jahanshahi F, Naderpour H, Kheyroddin A. Bond strength prediction of externally bonded reinforcement on groove method (EBROG) using MARS-POA. *Compos Struct* 2024;349–350:118532. <https://doi.org/10.1016/j.compstruct.2024.118532>.
- [28] Ma C, Wang S, Zhao J, Xiao X, Xie C, Feng X. Prediction of shear strength of RC deep beams based on interpretable machine learning. *Constr Build Mater* 2023;387:131640. <https://doi.org/10.1016/j.conbuildmat.2023.131640>.
- [29] Megahed K. Prediction and reliability analysis of shear strength of RC deep beams. *Sci Rep* 2024;14:14590.

- <https://doi.org/10.1038/s41598-024-64386-w>.
- [30] Keshavarz Z, Torkian H. Application of ANN and ANFIS models in determining compressive strength of concrete. *J Soft Comput Civ Eng* 2018;2:62–70.
- [31] Lee S-C. Prediction of concrete strength using artificial neural networks. *Eng Struct* 2003;25:849–57. [https://doi.org/10.1016/S0141-0296\(03\)00004-X](https://doi.org/10.1016/S0141-0296(03)00004-X).
- [32] Mohamed O, Kewalramani M, Ati M, Hawat W Al. Application of ANN for prediction of chloride penetration resistance and concrete compressive strength. *Materialia* 2021;17:101123. <https://doi.org/10.1016/j.mtla.2021.101123>.
- [33] Mater Y, Kamel M, Karam A, Bakhom E. ANN-Python prediction model for the compressive strength of green concrete. *Constr Innov* 2023;23:340–59. <https://doi.org/10.1108/CI-08-2021-0145>.
- [34] Chen L, Nouri Y, Allahyarsharahi N, Naderpour H, Rezazadeh Eidgahee D, Fakharian P. Optimizing compressive strength prediction in eco-friendly recycled concrete via artificial intelligence models. *Multiscale Multidiscip Model Exp Des* 2025;8:24. <https://doi.org/10.1007/s41939-024-00641-x>.
- [35] Nouri Y, Ghanbari MA, Fakharian P. An integrated optimization and ANOVA approach for reinforcing concrete beams with glass fiber polymer. *Decis Anal J* 2024;11:100479. <https://doi.org/10.1016/j.dajour.2024.100479>.
- [36] Paudel S, Pudasaini A, Shrestha RK, Kharel E. Compressive strength of concrete material using machine learning techniques. *Clean Eng Technol* 2023;15:100661. <https://doi.org/10.1016/j.clet.2023.100661>.
- [37] Eskandari-Naddaf H, Kazemi R. ANN prediction of cement mortar compressive strength, influence of cement strength class. *Constr Build Mater* 2017;138:1–11. <https://doi.org/10.1016/j.conbuildmat.2017.01.132>.
- [38] Lin C-J, Wu N-J. An ANN Model for Predicting the Compressive Strength of Concrete. *Appl Sci* 2021;11:3798. <https://doi.org/10.3390/app11093798>.
- [39] Moradi MJ, Khaleghi M, Salimi J, Farhangi V, Ramezaniyanpour AM. Predicting the compressive strength of concrete containing metakaolin with different properties using ANN. *Measurement* 2021;183:109790. <https://doi.org/10.1016/j.measurement.2021.109790>.
- [40] Noori F, Varae H. Nonlinear seismic response approximation of steel moment frames using artificial neural networks. *Jordan J Civ Eng* 2022;16.
- [41] ARIFUZZAMAN M. Application of Machine Learning for Predicting Concrete Strength: Ensembles vs. Instance-Based Algorithms in WEKA 2024. <https://doi.org/10.21203/rs.3.rs-4745693/v1>.
- [42] Saad S, Ishtiaque M, Malik H. Selection of most relevant input parameters using WEKA for artificial neural network based concrete compressive strength prediction model. 2016 IEEE 7th Power India Int. Conf., IEEE; 2016, p. 1–6. <https://doi.org/10.1109/POWERI.2016.8077368>.
- [43] Sharma N, Thakur MS, Sihag P, Malik MA, Kumar R, Abbas M, et al. Machine Learning Techniques for Evaluating Concrete Strength with Waste Marble Powder. *Materials (Basel)* 2022;15:5811. <https://doi.org/10.3390/ma15175811>.
- [44] Mattock AH. Strut-and-Tie Models for Dapped-End Beams. *Concr Int* 2012;34.
- [45] Quadri AI, Fujiyama C. Assessment of repaired reinforced concrete dapped-end beams exhibiting bond deterioration under static and cyclic loading. *Constr Build Mater* 2023;403:133070. <https://doi.org/10.1016/j.conbuildmat.2023.133070>.
- [46] Werner MP. Shear Design of Prestressed Concrete Stepped Beams. *PCI J* 1973;18:37–49. <https://doi.org/10.15554/pcij.07011973.37.49>.
- [47] Mattock AH, Chan TC. Design and Behavior of Dapped-End Beams. *PCI J* 1979;24:28–45. <https://doi.org/10.15554/pcij.11011979.28.45>.
- [48] Kashyap V, Alyaseen A, Poddar A. Supervised and unsupervised machine learning techniques for predicting mechanical properties of coconut fiber reinforced concrete. *Asian J Civ Eng* 2024;25:3879–99. <https://doi.org/10.1007/s42107-024-01018-8>.
- [49] Bajwa OI, Baluch HA, Saeed HA. Machine learning approach for predicting key design parameters in UAV conceptual design. *Ain Shams Eng J* 2024;15:102932. <https://doi.org/10.1016/j.asej.2024.102932>.
- [50] Ngamkhanong C, Alzabeebee S, Keawsawasvong S, Thongchom C. Performance of different machine learning techniques in predicting the flexural capacity of concrete beams reinforced with FRP rods. *Asian J*

- Civ Eng 2024;25:525–36. <https://doi.org/10.1007/s42107-023-00792-1>.
- [51] Pham A-D, Ngo N-T, Nguyen T-K. Machine learning for predicting long-term deflections in reinforce concrete flexural structures. *J Comput Des Eng* 2020;7:95–106. <https://doi.org/10.1093/jcde/qwaa010>.
- [52] Lu W, Lin I, Hwang S, Lin Y. Shear strength of high-strength concrete dapped-end beams. *J Chinese Inst Eng* 2003;26:671–80. <https://doi.org/10.1080/02533839.2003.9670820>.
- [53] Smith TC, Frank E. *Introducing Machine Learning Concepts with WEKA*, 2016, p. 353–78. https://doi.org/10.1007/978-1-4939-3578-9_17.
- [54] Vapnik VN. *The Nature of Statistical Learning Theory*. New York, NY: Springer New York; 2000. <https://doi.org/10.1007/978-1-4757-3264-1>.
- [55] Çevik A, Kurtuğlu AE, Bilgehan M, Gülşan ME, Albegmprli HM. Support Vector Machines in Structural Engineering: a Review. *J Civ Eng Manag* 2015;21:261–81. <https://doi.org/10.3846/13923730.2015.1005021>.
- [56] Ahmad S, Elahi A, Hafeez J, Fawad M, Ahsan Z. Evaluation of the shear strength of dapped ended beam. *Life Sci J* 2013;10:1038–44.
- [57] Abdallah MH, Thoeny ZA, Henedy SN, Al-Abdaly NM, Imran H, Bernardo LFA, et al. The Machine-Learning-Based Prediction of the Punching Shear Capacity of Reinforced Concrete Flat Slabs: An Advanced M5P Model Tree Approach. *Appl Sci* 2023;13:8325. <https://doi.org/10.3390/app13148325>.
- [58] Nguyen H, Vu T, Vo TP, Thai H-T. Efficient machine learning models for prediction of concrete strengths. *Constr Build Mater* 2021;266:120950. <https://doi.org/10.1016/j.conbuildmat.2020.120950>.
- [59] Üstün B, Melssen WJ, Buydens LMC. Facilitating the application of Support Vector Regression by using a universal Pearson VII function based kernel. *Chemom Intell Lab Syst* 2006;81:29–40. <https://doi.org/10.1016/j.chemolab.2005.09.003>.
- [60] Aswin M, Mohammed BS, Liew MS, Syed ZI. Shear Failure of RC Dapped-End Beams. *Adv Mater Sci Eng* 2015;2015:1–11. <https://doi.org/10.1155/2015/309135>.
- [61] Wang Q, Guo Z, Hoogenboom PCJ. Experimental investigation on the shear capacity of RC dapped end beams and design recommendations. *Struct Eng Mech* 2005;21:221–35. <https://doi.org/10.12989/sem.2005.21.2.221>.
- [62] Aswin M, Al-Fakih A, Syed Z, Liew M. Influence of Different Dapped-End Reinforcement Configurations on Structural Behavior of RC Dapped-End Beam. *Buildings* 2023;13:116. <https://doi.org/10.3390/buildings13010116>.
- [63] Huang P-C, Nanni A. Dapped-End Strengthening of Full-Scale Prestressed Double Tee Beams with FRP Composites. *Adv Struct Eng* 2006;9:293–308. <https://doi.org/10.1260/136943306776987010>.
- [64] Liem SK. Maximum shear strength of dapped-end or corbel 1983.
- [65] Fayed S, Madenci E, Özkılıç YO. Flexural Behavior of RC Beams with an Abrupt Change in Depth: Experimental Work. *Buildings* 2022;12:2176. <https://doi.org/10.3390/buildings12122176>.
- [66] Ghanem SY, Elgazzar H. Predicting the behavior of reinforced concrete columns confined by fiber reinforced polymers using data mining techniques. *SN Appl Sci* 2021;3:170. <https://doi.org/10.1007/s42452-020-04136-5>.
- [67] Gholamy A, Kreinovich V, Kosheleva O. Why 70/30 or 80/20 relation between training and testing sets: A pedagogical explanation 2018.
- [68] Kantardzic M. *Data mining: concepts, models, methods, and algorithms*. John Wiley & Sons; 2011.
- [69] Mansour MY, Dicleli M, Lee JY, Zhang J. Predicting the shear strength of reinforced concrete beams using artificial neural networks. *Eng Struct* 2004;26:781–99. <https://doi.org/10.1016/j.engstruct.2004.01.011>.
- [70] DAŞ O. Prediction of the natural frequencies of various beams using regression machine learning models. *Sigma J Eng Nat Sci – Sigma Mühendislik ve Fen Bilim Derg* 2023. <https://doi.org/10.14744/sigma.2023.00040>.
- [71] Upadhya A, Thakur MS, Sihag P. Predicting Marshall Stability of Carbon Fiber-Reinforced Asphalt Concrete Using Machine Learning Techniques. *Int J Pavement Res Technol* 2024;17:102–22. <https://doi.org/10.1007/s42947-022-00223-5>.
- [72] Quadri AI. Shear response of reinforced concrete deep beams with and without web opening. *Innov Infrastruct Solut* 2023;8:316. <https://doi.org/10.1007/s41062-023-01286-4>.